Theor Appl Climatol (2014) 117:475–484
DOI 10.1007/s00704-013-1022-x

ORIGINAL PAPER

Different influences of two types of El Niños on the Indian Ocean SST variations

Weichen Tao · Gang Huang · Kaiming Hu · Xia Qu · Guanhuan Wen · Yuanfa Gong

Received: 13 May 2013 / Accepted: 23 September 2013 / Published online: 6 October 2013

Abstract By comparing correlation of sea surface temperature (SST) and vertical circulation with canonical El Niño and El Niño Modoki, we find that El Niño Modoki has an effect on the Indian Ocean different from traditional El Niño. There exists obvious Indian Ocean basin mode (IOBM) after canonical El Niño, while insignificant SST anomalies exist in the Indian Ocean after El Niño Modoki. Anomalous downdraft and updraft appear over the eastern and western Indian Ocean, respectively, during canonical El Niño, while anomalous updraft is weak over the Indian Ocean during El Niño Modoki. Besides, the strength of El Niño Modoki is slightly weaker than that of canonical El Niño. According to previous studies, two mechanisms can explain IOBM after canonical El Niño: tropospheric temperature (TT) mechanism and ocean dynamics. However, both of them do not exist during El Niño Modoki. Comparing with the complicated oceanic processes, it is convenient to verify the observed TT anomalies and test the possible mechanism using the simple model. Therefore, we pay more attention on the question why TT mechanism does not work during El Niño Modoki. Using a linear barocinic model (LBM), we demonstrate that the strength of SST anomalies and cold SST anomalies in the eastern Pacific have an influence on TT anomalies. Especially, cold SST anomalies in the eastern Pacific cancel the effects of warm SST anomalies in the central Pacific on TT anomalies. It suggests that the SST anomalies in the eastern Pacific are important for the TT mechanism in two types of El Niño.

W. Tao · K. Hu · X. Qu · G. Wen
Center for Monsoon System Research, Institute of Atmospheric Physics, Chinese Academy of Sciences, Beijing, China

W. Tao · Y. Gong
Chengdu University of Information Technology, Chengdu, China

G. Huang (✉)
Key Laboratory of Regional Climate–Environment for East Asia, Institute of Atmospheric Physics, Chinese Academy of Sciences, Beijing 100029, China
e-mail: hg@mail.iap.ac.cn

G. Huang
Collaborative Innovation Center on Forecast and Evaluation of Meteorological Disasters, Nanjing, China

G. Wen
University of Chinese Academy of Sciences, Beijing, China

1 Introduction

The interannual sea surface temperature (SST) variation in the Indian Ocean exerts a substantial influence on the surrounding regions. The first leading mode of the interannual Indian Ocean SST variability features a basin-wide warming or cooling, known as Indian Ocean Basin Mode (IOBM). When the IOBM is in the warming state, warm tropospheric Kelvin wave is triggered, which can contributes to the anomalous anticyclone over the Northwest Pacific (NWP) via the "capacitor effect" (Xie et al. 2009), the meridional displacement of the East Asian jet (EAJ) (Qu and Huang 2012b) and the intensity of the South Asia high (SAH; Qu and Huang 2012a), and thus affect the East Asian climate, including summer rainfall (Xie et al. 2010), typhoon (Du et al. 2011), high temperature extremes (Hu et al. 2011, 2012a, b) and so on.

The Indian Ocean basin-wide warming generally develops during the winter when El Niño matures, reaches its peak in the following spring (Alexander et al. 2002; Lau and Nath 2003; Schott et al. 2009), and persists into the summer (Du et al. 2009). Numerous studies have investigated the mechanisms for the formation of basin-wide warming in the Indian Ocean. Lau (1997) showed that El Niño-induced anomalous atmospheric circulation can cause IOBM through reducing surface evaporation and increasing incoming short wave radiation, which is known as "atmospheric bridge" mechanism (Klein

et al. 1999). The spread of tropospheric temperature (TT) anomalies associated with the propagation of El Niño-induced equatorial planetary waves from the eastern Pacific to the remote Tropics is the important process in such atmospheric bridge, which is also called the TT mechanism (Chiang and Sobel 2002; Chiang and Lintner 2005). Klein et al. (1999) reported that net surface heat flux anomalies can explain most of the tropical Indian Ocean (TIO) warming, but the tropical southwestern Indian Ocean (SWIO) is an exception, suggesting that ocean dynamics is important there, which is further proved in model study (Lau and Nath 2000). Masumoto and Meyers (1998) reported that there are anticyclonic wind anomalies over the south TIO during the developing and mature phases of El Niño, which cause the downwelling Rossby wave. The Rossby wave propagates to the SWIO where the thermocline is shallow and the Rossby wave is responsible for the SST rising there (Xie et al. 2002). After the warming of SWIO, the SST anomalies there excite an equatorially antisymmetry pattern of wind anomalies as a key to the IOBM persisting into summer by reducing the prevailing southwest monsoon during spring and so as to the latent heat flux (Du et al. 2009).

Recently, a new type of El Niño event has been reported (literature). Comparing to canonical El Niño, the new type of El Niño is characterized by warming in the central equatorial Pacific and cooling in two sides — called El Niño Modoki. Previous studies have examined the SST variability in the TIO associated with canonical El Niño and El Niño Modoki (Ashok et al. 2007; Chowdary and Gnanaseelan 2007; Wu et al. 2012; Chakravorty et al. 2013), but very few studies examined the difference between the influences of two types of El Niño on the Indian Ocean SST. Besides, a better understanding of the influences of two types of El Niño on the Indian Ocean is important for the prediction of the Indian Ocean SST anomalies and the associated climate anomalies. Therefore, two questions arise: one is what are the different influences of two types of El Niño on the Indian Ocean SST? The other is what mechanisms cause the differences?

The rest of the article is organized as follows. Section 2 describes the model, data and methods. Section 3 describes the SST anomaly pattern of canonical El Niño and El Niño Modoki, and compares the different influences of two types of El Niños on the Indian Ocean based on observations. Section 4 investigates the possible mechanisms for the influences of two types of El Niños on the Indian Ocean by using a Linear Baroclinic Model (LBM). Section 5 presents a summary and discussions.

2 Model, data and methods

2.1 Model

The LBM described by Watanabe and Kimoto (2000) is used. It is a global, time-dependent, primitive-equation model, linearized about the observed climatology derived from the National Centers for Environmental Prediction/National Center for Atmospheric Research (NCEP–NCAR) reanalysis for 1958–97. Its resolution is T21 in the horizontal and 20 sigma levels in the vertical. The model employs diffusion (horizontal and vertical), Rayleigh friction, and Newtonian damping. The latter two terms have a time scale of $(1\ \text{day})^{-1}$ for $\sigma \geq 0.9$ and $\sigma \leq 0.03$, while $(30\ \text{day})^{-1}$ is used elsewhere. In this study, we use the dry version of the LBM forced by diabatic heating anomalies, which should be proportional to the observed precipitation anomalies. The horizontal shape of the heating is elliptical and the heating is imposed on winter (December, January, February [DJF]) mean state (from the NCEP–NCAR reanalysis). The vertical heating profile is gamma with a maximum heating at $\sigma = 0.45$.

2.2 Data and analysis methods

In this study, the SST used here is from the Hadley Centre Sea ICE and Sea Surface Temperature dataset (HadISST; Rayner et al. 2003). It has a 1°×1° horizontal resolution and covers the period from January 1870 to the present. Atmospheric circulation monthly data are from the NCEP/NCAR reanalysis product (Kalnay et al. 1996). This dataset has a 2.5°×2.5° horizontal resolution and extends from 1,000 to 10 hPa with 17 pressure levels in vertical. We also utilize the sea surface height (SSH) data derived from the Simple Ocean Data Assimilation (SODA) product for the period January 1958 through December 2008 on a 0.5°×0.5° grid (Carton et al. 2005; Carton and Giese 2008). The data in the present analysis cover the period January 1951 to December 2010 except for the SODA data that span the period from January 1958 through December 2008. The monthly mean climatology is first calculated for the study period. Then, interannual anomalies are computed as the departure from this climatology. And the linear trend has been removed from all the data.

Hereafter, any month in the El Niño onset year is identified by suffix (0), whereas any month in the El Niño decay year is identified by suffix (1). The IOBM index is defined as SST anomalies averaged over the TIO (40°–110°E, 20°S–20°N). The Niño3 index is defined as SST anomalies averaged over the eastern equatorial Pacific (5°S–5°N, 150°–90°W). And EMI index is defined as $\text{EMI} = [\text{SSTa}]_A - 0.5 \times [\text{SSTa}]_B - 0.5 \times [\text{SSTa}]_C$, where subscript A, B and C represent the area-averaged SST anomalies in region A (165°E–140°W, 10°S–10°N), B (110°W–70°W, 15°S–5°N) and C (125°E–145°E, 10°S–20°N), respectively (Ashok et al. 2007). We also use the statistical methods such as empirical orthogonal function (EOF) analysis and correlation analysis. The significance levels for correlation analysis are evaluated with the standard two-tailed Student's t-test.

3 Different influences of two types of El Niños on the Indian Ocean

3.1 The leading two modes of tropical Pacific SST variability

The leading two EOF modes of seasonal mean SST anomalies in the tropical Pacific region (20°S–20°N, 110°E–80°W) during winter (DJF) are showed in Fig. 1. These two modes contribute to 66.2 % and 9.4 % of total SST variance for the period 1951 to 2010, respectively. The first EOF pattern (Fig. 1a) is the canonical El Niño pattern (Rasmusson and Carpenter 1982), and the second (Fig. 1b) shows the El Niño Modoki, resembling the results of Ashok et al. (2007). The variances explained by the first two EOF patterns are well separated according to North et al. (1982), so it is convincible that EOF1 and EOF2 represent different modes of tropical Pacific SST variability. The time series of principal components (PCs) corresponding to EOF1 and EOF2 are presented in Fig. 1c and d. The correlation coefficients between PC1 and Niño3 index, PC2 and EMI are very high, reaching 0.99 and 0.74, respectively. This indicates that EOF1 and EOF2 well represent canonical El Niño and El Niño Modoki, respectively. For convenience, we define PC1 as the canonical El Niño index, and PC2 as the El Niño Modoki index.

3.2 The correlation of two types of El Niños with the Indian Ocean

3.2.1 Characteristics of two types of El Niño

In order to better understand the relationship of two types of El Niños with the Indian Ocean SST variations, we calculated the correlation of various variables with PCs. Figure 2 presents the correlation of SST anomalies with PCs from winter to summer. There is a substantial difference between the canonical El Niño (Fig. 2a–c) and El Niño Modoki (Fig. 2d–f). Firstly, anomalous SST distribution shows the different characteristics between the canonical El Niño and El Niño Modoki in the equatorial Pacific region. Secondly, the obvious IOBM follows the canonical El Niño, while insignificant SST anomalies are found in the Indian Ocean after El Niño Modoki. Thirdly, the intensity of El Niño Modoki is slightly weaker than that of canonical El Niño, as is shown in Fig. 1a and b.

Anomalous Walker circulation responses display distinct features when two types of El Niño occur (Fig. 3). The structure of vertical circulations during DJF (0) and MAM (March, April, May) (1) is clear, while the structure during JJA (June, July, August) (1) cannot be clearly distinguished. In the Pacific region, typical anomalous Walker circulations are observed during canonical El Niño with updraft over the central-eastern Pacific and downdraft over the western Pacific (Fig. 3a, b). The anomalous Walker circulations also show a single cell pattern during El Niño Modoki; however, there is updraft over the central Pacific and downdraft over the eastern Pacific (Fig. 3d, e). Moreover, the downdraft over the western Pacific is not clear comparing with the Fig. 7 of Weng et al. (2009), which may be due to the different El Niño Modoki indexes and statistical analysis methods. The biggest differences in two types of El Niños are in the position of updraft and downdraft over the Pacific Ocean. Additionally, over the Indian Ocean region, there are downdraft over the eastern Indian Ocean and updraft over the western Indian Ocean during canonical El Niño (Fig. 3a, b), while the overall weak updraft over the Indian Ocean during El Niño Modoki (Fig. 3d–f). These vertical motion differences can be linked to SST anomalies in the different domain of the equatorial Pacific through the Walker circulation. In turn, they lead to different net surface heat flux variations and then different SST variations over the remote ocean (Lau 1997; Goddard and Graham 1999; Chiang et al. 2000; Chiang and Sobel 2002).

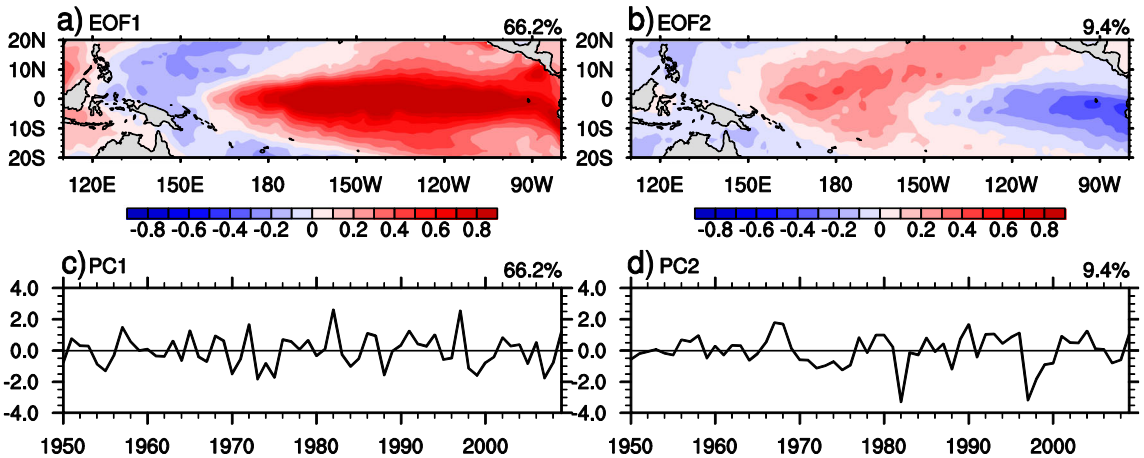

Fig. 1 The top two EOF modes (*upper panels*, **a** and **b**) and corresponding principal components (*bottom panels*, **c** and **d**) for the tropical Pacific SSTa (1951–2010) during boreal winter (DJF)

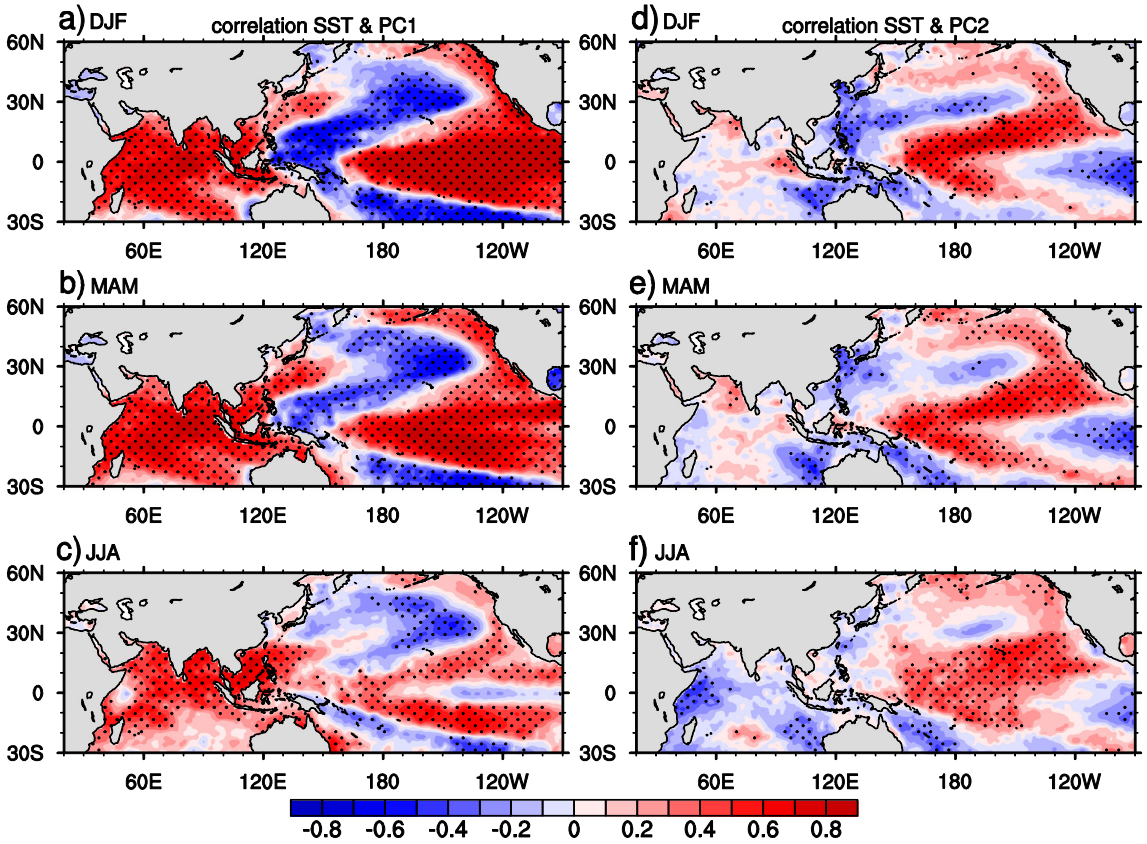

Fig. 2 Correlation of SST anomalies with PC1 during DJF (0), MAM (1), JJA (1) (*left panels*, **a**–**c**), and the same with PC2 (*right panels*, **d**–**f**). *Dots* indicate that significant level reaches 95 %

3.2.2 TT mechanism

Free atmosphere of the tropical eastern Pacific warms with the SST increase, and this is to be followed by consistent warming throughout the tropical regions around the world in the following 1–2 months (Charney 1963; Wallace 1992; Sobel and Bretherton 2000). Atmospheric wave is the most effective way to spread the warm anomalies in free atmosphere (Su et al. 2003), so TT mechanism is proposed afterward (Chiang and Sobel 2002).

Chiang and Sobel (2002) indicate that the TT mechanism is more or less the Walker circulation mechanism, just posed in a different way from the "atmospheric bridge" mechanism. Figure 4 presents lead–lag correlation of mean 1,000–200 hPa TT with PC1. During the canonical El Niño, persistent warming in the east Pacific, through convection and moist adjustment, heats the whole tropospheric column there, and forms the Matsuno–Gill pattern (Matsuno 1966; Gill 1980) in TT. As time goes on, the warm pattern develops and extends to the east by forcing the Kelvin wave eastward and affects the climate of other remote regions. Figure 5 shows the same correlation, except for PC2. A huge difference exists between the TT responses to the canonical El Niño and the El Niño Modoki. During the El Niño Modoki, both the strength and range of the TT anomalies are weaker and less obvious than those during the canonical El Niño. In addition to the small range of weak TT anomalies over the central Pacific, there are no apparent TT anomalies in other regions of the world, so there are no obvious Kelvin wave characteristics.

Overall, during the canonical El Niño, there exist TT anomalies over the global tropical strip, so the TT mechanism works and it is also one of the crucial factors for the responses of SST anomalies in the Indian Ocean. In comparison, during the El Niño Modoki, there do not exist apparent TT anomalies, so no obvious impact can be detected on the Indian Ocean. Conspicuously, TT anomalies are caused by abnormal SST in the tropical Pacific, and they depend upon whether the anomalous SST pattern is that of canonical El Niño or El Niño Modoki. In addition, the location and intensity of SST anomalies are different in two types of El Niños, and El Niño Modoki has cold SST anomalies in the eastern Pacific. Therefore, we may ask if the location and intensity of SST anomalies or cold SST anomalies in the eastern Pacific influence the formation of TT anomalies, then influence the climate of the Indian Ocean. We will use LBM to discuss these topics in Section 4.

3.2.3 Ocean dynamics

TT mechanism is on the view of atmosphere affecting ocean, but in some regions of the ocean, oceanic processes play an

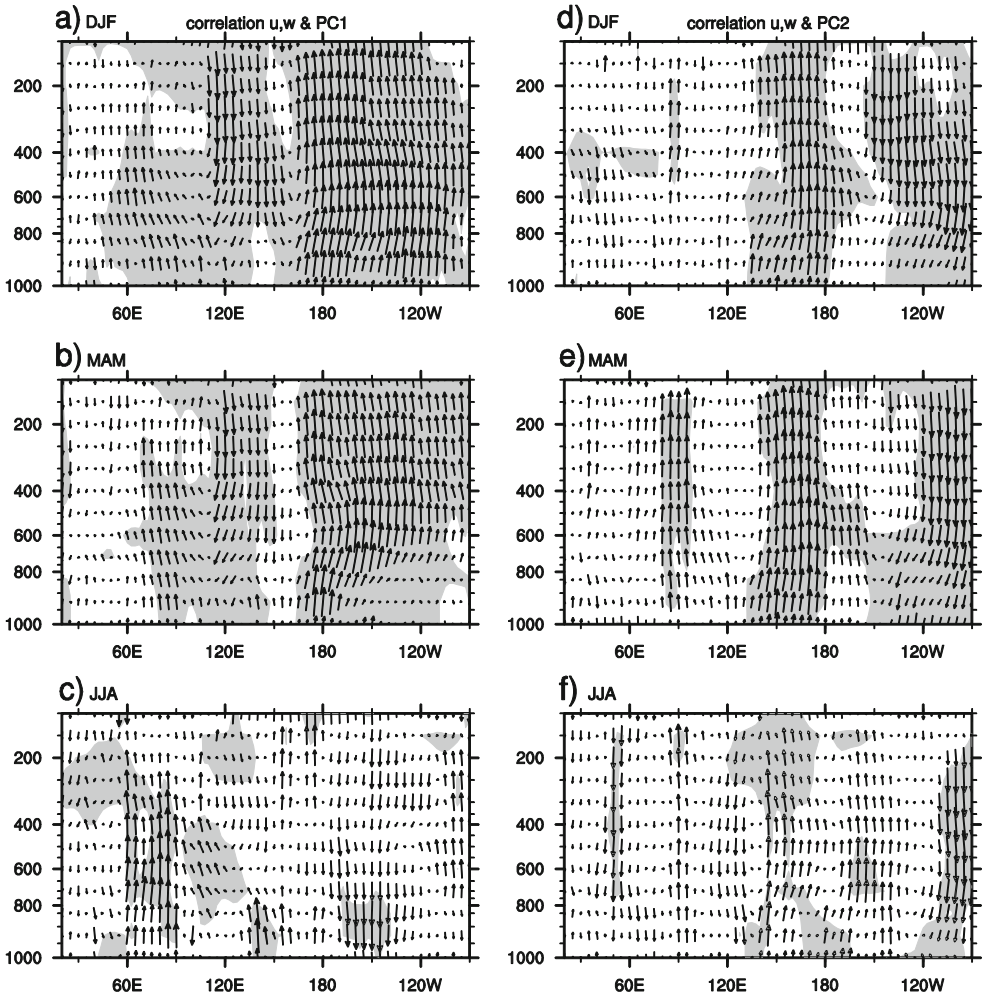

Fig. 3 Correlation of *u*, *w* anomalies with PC1 during DJF (0), MAM (1), JJA (1) (*left panels*, **a**–**c**), and the same with PC2 (*right panels*, **d**–**f**). *Shadings* indicate significant level reaches 95 %

important role in the development of SST anomalies. Klein et al. (1999) reported the absence of positive net surface heat flux anomalies in the tropical SWIO near Madagascar, suggesting that ocean dynamics is important there. Thereafter, Xie et al. (2002) posed that there was a westward-propagating downwelling Rossby wave in the SWIO forced by the anomalous easterlies in the equatorial Indian Ocean, which induces positive SST anomalies there. This is another crucial factor for the IOBM, so it is necessary to compare the differences between the oceanic processes of two types of El Niños.

Figure 6 shows the lead–lag correlation of SSH (averaged in 5°S–5°N) with PC1 and PC2 as a function of longitude and calendar month. An equatorial Kelvin wave propagates slowly all the way to the east in the Pacific. This Kelvin wave is in favor of the development of El Niño that reaches its peak around winter (DJF). After the mature phase of El Niño, another Rossby wave caused by El Niño propagates westward to the SWIO where the mean thermocline is shallow. The Rossby wave deepens thermocline, and raises SST there. After the warming of SWIO, the SST anomalies there excite an equatorially antisymmetry pattern of wind anomalies (Fig. 7a). The wind anomalies reduce the prevailing southwest monsoon during spring and so as to the latent heat flux. As a result, the Indian Ocean basin-wide warming sustains and can even persist into summer (Fig. 7a). Compared with the canonical El Niño, however, no significant wave propagation exists in the Indian Ocean (Fig. 8b). Consequently, no obvious wind anomalies or SST anomalies appear in the Indian Ocean after El Niño Modoki (Fig. 7b).

As mentioned above, during El Niño Modoki, neither the TT mechanism nor ocean dynamics exist in the Indian Ocean. However, ocean dynamics are extremely complicated, containing a variety of linear and nonlinear processes. Thus, it is difficult to explain the absent oceanic processes in the Indian Ocean without using the sophisticated coupled models. In contrast, the TT mechanism is forced by the abnormal heat source over the ocean region. It is convenient to verify the observations and test the possible mechanism using the simple model. Therefore, we pay more attention on the question why El Niño Modoki does not generate TT mechanism.

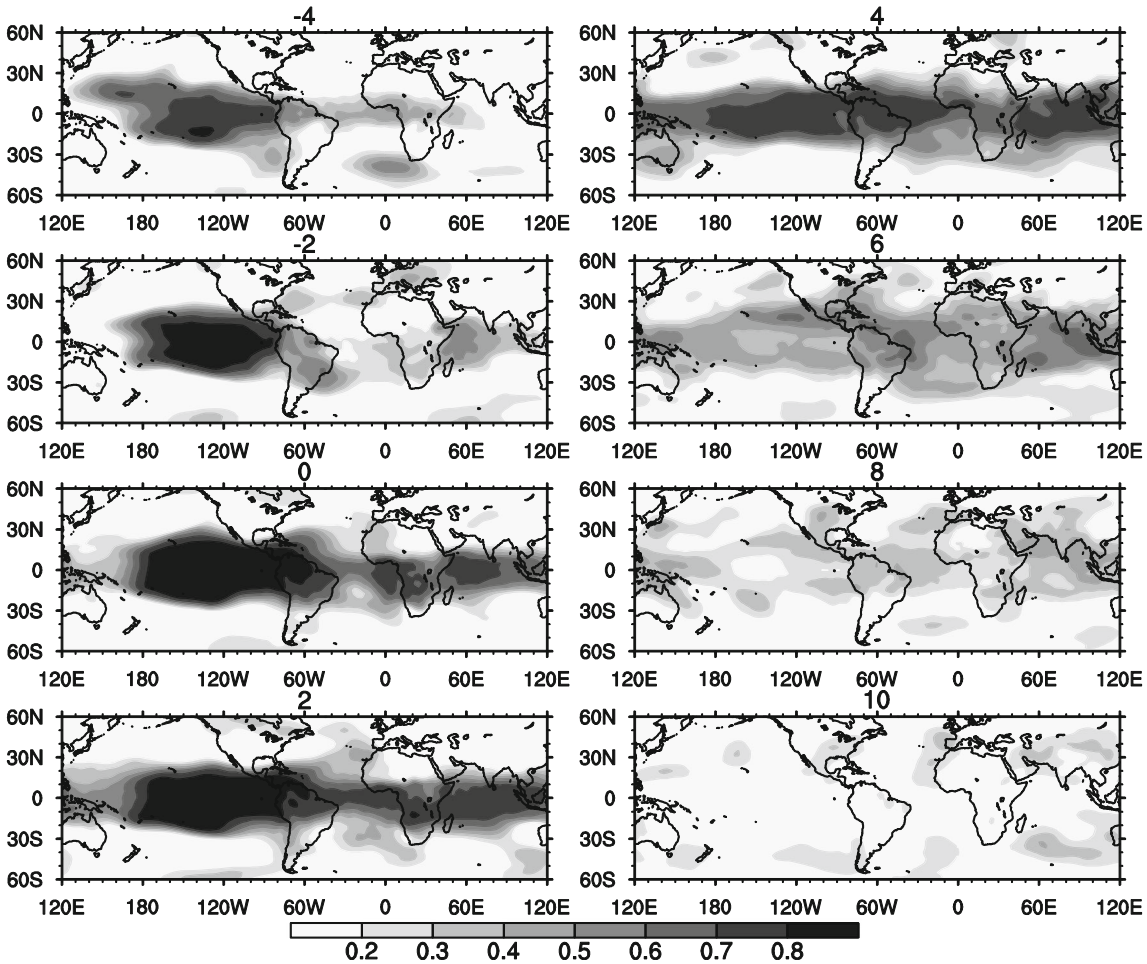

Fig. 4 Lead–lag correlation of mean 1,000–200 hPa tropospheric temperature (*TT*) with PC1. The *number above each panel* indicates the lead or lag in months: 4 implies TT leads PC1 4 months, 2 implies TT leads PC1 2 months, and so on

4 Solutions to the dry LBM

The LBM solutions provide a straightforward view of the basic dynamics. We use this model to illustrate how the location and intensity of SST anomalies or cold SST anomalies in the eastern Pacific influence the formation of TT anomalies. Moreover, the observed anomalous precipitation patterns during two types of El Niños (Ashok et al. 2007; Weng et al. 2009) are similar to the anomalous SST pattern. Therefore, it is reasonable to use the dry version of the LBM forced by the idealized diabatic heating here.

4.1 The experimental design

Figure 8a, b and c shows the three column integrated heating profiles that are used to force the dry version of the LBM. To represent the heating anomalies of canonical El Niño, we put the idealized diabatic heating in the tropical eastern Pacific (center at 0° and 135°W). The zonal and meridional extent of heating anomalies are 55° and 10°, respectively (Fig. 8a). To represent the heating anomalies only in the tropical central Pacific, we put the center of the idealized diabatic heating at 0° and 170°W. The zonal and meridional extent of heating anomalies are 30° and 10°, respectively (Fig. 8b). To represent the heating anomalies of El Niño Modoki, we not only imposed the heating anomalies in the tropical central Pacific as before, but also imposed another diabatic heating in the tropical eastern Pacific, centered near 0° and 105°W, with the zonal and meridional extent of heating anomalies of 25° and 10°, respectively (Fig. 8c). The LBM is integrated for 50 days. The response reaches the equilibrium after 15 days, so we analyze the last 30 days.

4.2 Result

The responses of TT anomalies to the heating (Fig. 8a–c) are shown in Fig. 8d–f. In the canonical El Niño forcing scenario (Fig. 8d), the significant TT anomalies are over the global tropical strip, consistent with the observation in Fig. 4. This illustrates that heating in the tropical eastern Pacific affects

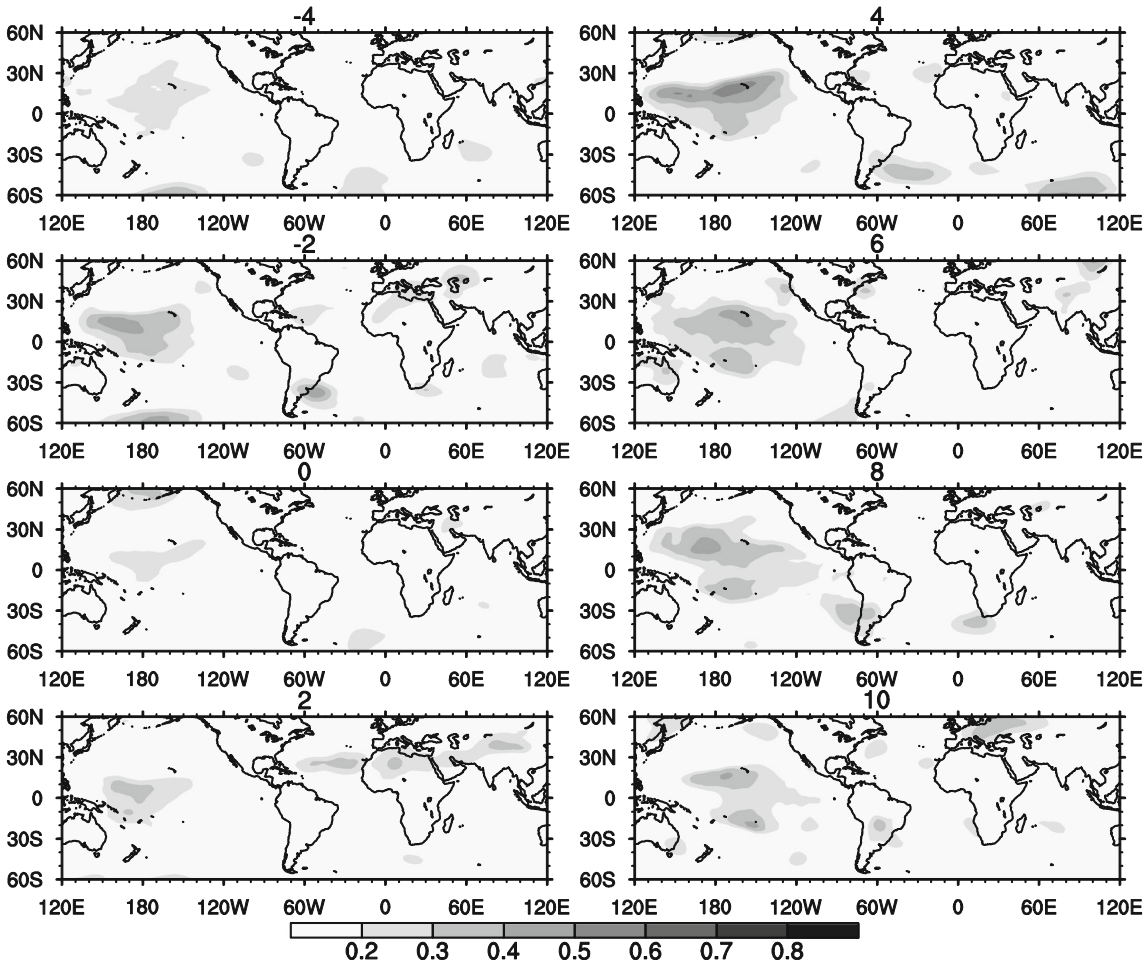

Fig. 5 Same as Fig 6, but for PC2

remote regions through the TT mechanism. In the tropical central Pacific forcing scenario (Fig. 8e), there also exist TT anomalies over the global tropical strip, but the intensity of the TT anomalies is weaker. One factor for the different response of TT anomalies is the strength of heating. Obviously, the central intensity of heating in Fig. 8a and b are the same, but the range of heating is bigger in Fig. 8a than in Fig. 8b. For El Niño Modoki forcing scenario (Fig. 8f), almost no obvious TT anomalies appear. The only difference between the heating of Fig. 8b and c is the negative heating anomalies in the tropical

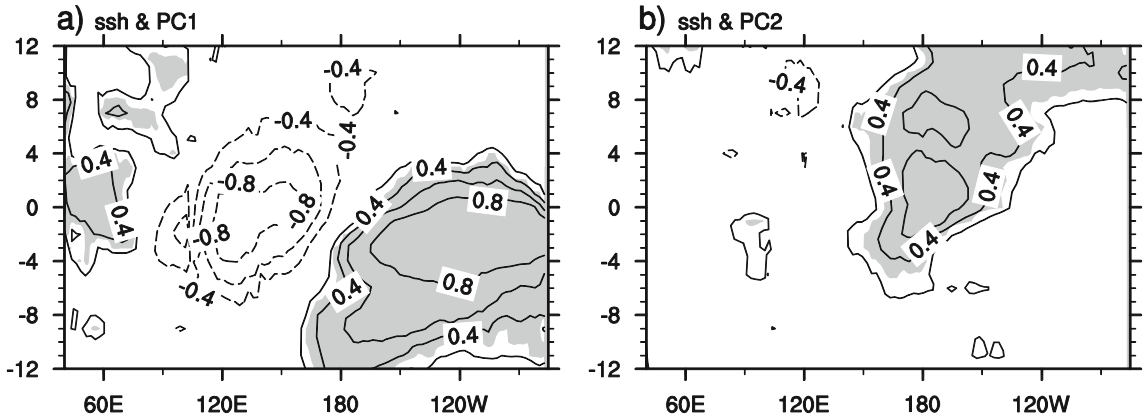

Fig. 6 Lead–lag correlation of SSH, averaged in 5°S–5°N, with **a** PC1 and **b** PC2 as a function of longitude and calendar month. *Shadings* indicate the correlation coefficient is greater than 0.6. *Shadings* indicate that significant level reaches 95 %

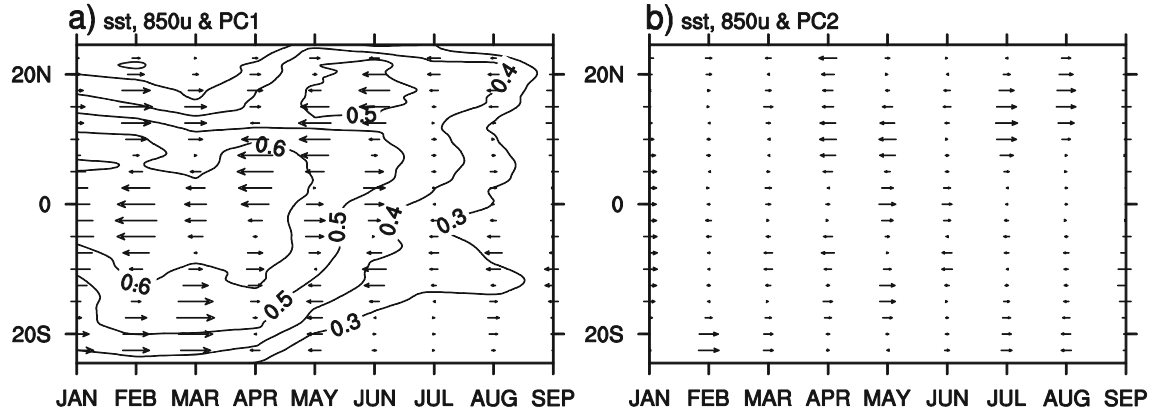

Fig. 7 Correlation of SST anomalies (contour) and 850 hPa wind anomalies (vector), averaged in 40°E–100°E, with **a** PC1 and **b** PC2 as a function of latitude and calendar month

eastern Pacific. Compared to the positive heating anomalies in the central Pacific, the negative heating anomalies have an opposite effect on the TT anomalies. So the TT anomalies caused by positive heating are offset by negative heating. Wu et al. (2010) also proposed that the TT anomalies rely on the SST anomalies in other regions, and negative SST anomalies in the tropical Atlantic Ocean may cancel the TT increase induced by positive SST anomalies in the equatorial Pacific.

The response of vertical motion to the heating (Fig. 8a–c) is shown in Fig. 8g–i. There are strong updrafts over the eastern and central Pacific (Fig. 8g and h), respectively. Accordingly, there are downdrafts in the Indian Ocean, although they are very weak. However, when a single cell exists in the central and eastern Pacific (Fig. 8i), there is no obvious vertical motion over the Indian Ocean, indicating that the negative heating anomalies have an opposite effect. We also note that the vertical structure of Fig. 8g and i is similar to that of Fig. 3a and d, respectively. As a result, the negative heating anomalies, or the cold SST anomalies in the eastern Pacific are the reason why the TT mechanism does not work in El Niño

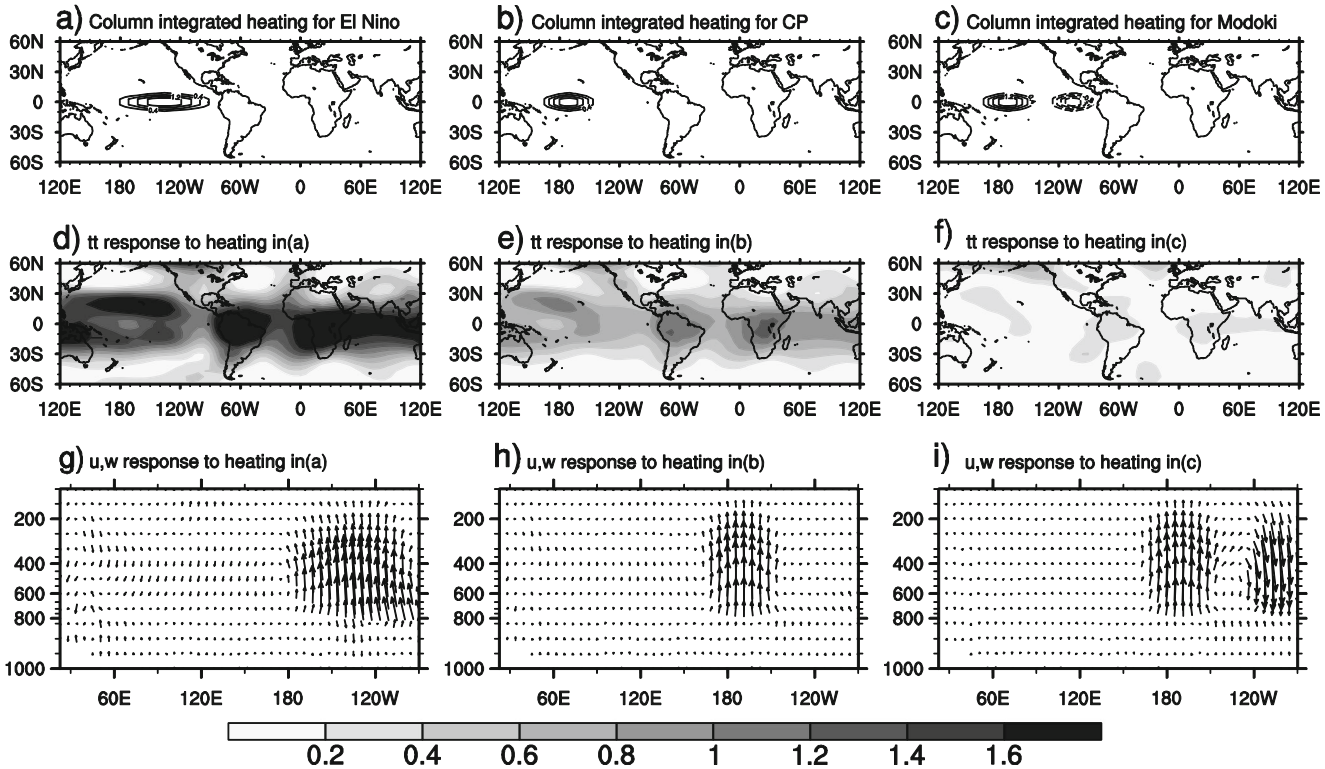

Fig. 8 Vertical column-integrated diabatic heating anomalies (K day^{-1}) imposed for **a** the canonical El Niño, **b** the tropical central Pacific and **c** El Niño Modoki. **d**, **e**, **f** The TT anomalies response to the heating in **a**, **b**, **c**, respectively. **g**, **h** and **i** are same as **d**, **e** and **f**, but for u, w wind anomalies

Modoki. Therefore, we initially conclude that the presence of SST anomalies in the eastern Pacific is an important reason for the differences of the Indian Ocean SST variations in two types of El Niño.

5 Summary and discussion

Based on the results of statistical analysis, we have compared the characteristics of two types of El Niños and their effect on the Indian Ocean, as well as the mechanism of their effect on the Indian Ocean.

The leading two EOF modes of SST anomalies in the tropical Pacific during winter (DJF) represent the canonical El Niño pattern and El Niño Modoki pattern, respectively. For the canonical El Niño, the SST anomaly pattern shows a "negative–positive" zonal dipole structure in the tropical Pacific. For the El Niño Modoki, the SST anomaly pattern shows a "negative–positive–negative" zonal tripole structure. And the correlation coefficients between PC1 and Nino3, PC2 and EMI are very high, reaching 0.99 and 0.74, respectively.

There exists obvious IOBM after canonical El Niño, while the SST change is insignificant after El Niño Modoki. Moreover, the strength of El Niño Modoki is slightly weaker than that of the canonical El Niño. The vertical motion also shows a huge difference between the two types of El Niño over the Indian Ocean. During canonical El Niño, there is downdraft over the eastern Indian Ocean and updraft over the western Indian Ocean, while the updraft over the Indian Ocean is weak during El Niño Modoki.

On the view of the atmosphere affecting ocean, we can use the TT mechanism to explain the different influences on the Indian Ocean. During the canonical El Niño, there is a Matsuno–Gill pattern (Matsuno 1966; Gill 1980) in TT. This warm pattern develops and extends to the east by forcing the Kelvin wave eastward, as proposed by Chiang and Sobel (2002). However, both the strength and range of the TT anomalies are weaker and less obvious in the El Niño Modoki. Moreover, there are no obvious Kelvin wave characteristics.

On the view of internal oceanic processes, after the mature phase of El Niño, we can see that the El Niño-induced Rossby wave propagates westward to the SWIO and induces SST anomalies there. However, during the El Niño Modoki, there is no significant wave propagation in the Indian Ocean. Consequently, no SST anomalies appear there after El Niño Modoki.

However, ocean dynamics contain a variety of linear and nonlinear processes. It is difficult to explain the absent oceanic processes in the Indian Ocean without using the sophisticated coupled models. In contrast, the TT mechanism is forced by the abnormal heat source over the ocean region. It is convenient to verify the observations and test the possible mechanism using the simple model. Therefore, we pay more attention on the question why El Niño Modoki does not generate TT mechanism. Results of an LBM with imposed heating demonstrate that the strength of SST anomalies and cold SST anomalies in the eastern Pacific have an influence on TT anomalies. In particular, the cold SST anomalies have an effect on TT anomalies opposite to the warm SST anomalies in the central Pacific. This suggests that the anomalous SST pattern in the tropical Pacific is most important for the TT mechanism in two types of El Niños.

This study focused on the different influences of two types of El Niños on the Indian Ocean SST. On one hand, El Niño Modoki has a different structure and strength of SST anomalies from canonical El Niño. On the other hand, relative to canonical El Niño, the TT mechanism does not work and there is no oceanic process during El Niño Modoki. However, IOBM is partly caused by net surface heat flux, which, in turn, is related to cloud/precipitation/wind changes (Klein et al. 1999). And we note that the TT mechanism can only explain the general temperature structure change, but it does not directly relate to cloud/precipitation/wind changes. More relevant is the cloud/precipitation/wind changes that contribute to surface heat fluxes. Therefore, identification of the different impacts on the Indian Ocean SST changes between two types of El Niños calls for more detailed research on cloud/precipitation/wind changes over the Indian Ocean, and further studies should focus on these aspects as well as the absent oceanic processes by sophisticated models.

Acknowledgments This work was supported by the National Basic Research Program of China (2012CB955604 and 2011CB309704), the Strategic Priority Research Program of the Chinese Academy of Sciences (XDA05090402), and the National Natural Science Foundation of China (41275083). The authors thank Prof. Wu Renguang and two anonymous reviewers as well as editors for their useful comments.

References

Alexander MA, Blade I, Newman M, Lanzante JR, Lau NC, Scott JD (2002) The atmospheric bridge: the influence of ENSO teleconnections on air–sea interaction over the global oceans. J Clim 15(16):2205–2231. doi:10.1175/1520-0442(2002)015<2205:tabtio>2.0.co;2

Ashok K, Behera SK, Rao SA, Weng H, Yamagata T (2007) El Niño Modoki and its possible teleconnection. J Geophys Res 112(C11), C11007

Carton JA, Giese BS (2008) A reanalysis of ocean climate using Simple Ocean Data Assimilation (SODA). Mon Weather Rev 136(8):2999–3017. doi:10.1175/2007mwr1978.1

Carton JA, Giese BS, Grodsky SA (2005) Sea level rise and the warming of the oceans in the Simple Ocean Data Assimilation (SODA) ocean reanalysis. J Geophys Res-Oceans 110(C9):C09006 doi: 10.1029/2004jc002817

Chakravorty S, Chowdary JS, Gnanaseelan C (2013) Spring asymmetric mode in the tropical Indian Ocean: role of El Niño and IOD. Clim Dyn 40(5–6):1467–1481. doi:10.1007/s00382-012-1340-1

Charney JG (1963) A note on large-scale motions in the tropics. J Atmos Sci 20(6):607–609. doi:10.1175/1520-0469(1963)020<0607:anolsm>2.0.co;2

Chiang JCH, Lintner BR (2005) Mechanisms of remote tropical surface warming during El Niño. J Clim 18(20):4130–4149. doi:10.1175/jcli3529.1

Chiang JCH, Sobel AH (2002) Tropical tropospheric temperature variations caused by ENSO and their influence on the remote tropical climate. J Clim 15(18):2616–2631. doi:10.1175/1520-0442(2002)015<2616:tttvcb>2.0.co;2

Chiang JCH, Kushnir Y, Zebiak SE (2000) Interdecadal changes in eastern Pacific ITCZ variability and its influence on the Atlantic ITCZ. Geophys Res Lett 27(22):3687–3690. doi:10.1029/1999gl011268

Chowdary JS, Gnanaseelan C (2007) Basin-wide warming of the Indian Ocean during El Niño and Indian Ocean dipole years. Int J Climatol 27(11):1421–1438. doi:10.1002/joc.1482

Du Y, Xie SP, Huang G, Hu K (2009) Role of air–sea Interaction in the long persistence of El Niño-induced North Indian Ocean warming. J Clim 22(8):2023–2038

Du Y, Yang L, Xie SP (2011) Tropical Indian Ocean influence on Northwest Pacific tropical cyclones in summer following Strong El Niño. J Clim 24(1):315–322. doi:10.1175/2010jcli3890.1

Gill AE (1980) some simple solutions for heat-induced tropical circulation. Q J R Meteorol Soc 106(449):447–462. doi:10.1256/smsqj.44904

Goddard L, Graham NE (1999) Importance of the Indian Ocean for simulating rainfall anomalies over eastern and southern Africa. J Geophys Res-Atmos 104(D16):19099–19116. doi:10.1029/1999jd900326

Hu K, Huang G, Huang R (2011) The impact of tropical Indian Ocean variability on summer surface air temperature in China. J Clim 24(20):5365–5377

Hu K, Huang G, Qu X, Huang R (2012a) The impact of Indian Ocean variability on high temperature extremes across the southern Yangtze River valley in late summer. Adv Atmos Sci 29(1):91–100

Hu K, Huang G, Wu R (2012b) A strengthened influence of ENSO on August high temperature extremes over the Southern Yangtze River valley since the Late 1980s. J Clim 26(7):2205–2221. doi:10.1175/jcli-d-12-00277.1

Kalnay E, Kanamitsu M, Kistler R, Collins W, Deaven D, Gandin L, Iredell M, Saha S, White G, Woollen J, Zhu Y, Chelliah M, Ebisuzaki W, Higgins W, Janowiak J, Mo KC, Ropelewski C, Wang J, Leetmaa A, Reynolds R, Jenne R, Joseph D (1996) The NCEP/NCAR 40-year reanalysis project. Bull Am Meteorol Soc 77(3):437–471. doi:10.1175/1520-0477(1996)077<0437:tnyrp>2.0.co;2

Klein SA, Soden BJ, Lau N-C (1999) Remote sea surface temperature variations during ENSO: evidence for a tropical atmospheric bridge. J Clim 12(4):917–932. doi:10.1175/1520-0442(1999)012<0917:rsstvd>2.0.co;2

Lau NC (1997) Interactions between global SST anomalies and the midlatitude atmospheric circulation. Bull Am Meteorol Soc 78(1):21–33. doi:10.1175/1520-0477(1997)078<0021:ibgsaa>2.0.co;2

Lau NC, Nath MJ (2000) Impact of ENSO on the variability of the Asian–Australian monsoons as simulated in GCM experiments. J Clim 13(24):4287–4309. doi:10.1175/1520-0442(2000)013<4287:ioeotv>2.0.co;2

Lau NC, Nath MJ (2003) Atmosphere–ocean variations in the Indo-Pacific sector during ENSO episodes. J Clim 16(1):3–20. doi:10.1175/1520-0442(2003)016<0003:aoviti>2.0.co;2

Masumoto Y, Meyers G (1998) Forced Rossby waves in the southern tropical Indian Ocean. J Geophys Res 103(C12):27589–27602. doi:10.1029/98jc02546

Matsuno T (1966) Quasi-geostrophic motions in the equatorial area. J Meteorol Soc Jpn 44(1):25–43

North GR, Bell TL, Cahalan RF, Moeng FJ (1982) Sampling errors in the estimation of empirical orthogonal functions. Mon Weather Rev 110(7):699–706. doi:10.1175/1520-0493(1982)110<0699:seiteo>2.0.co;2

Qu X, Huang G (2012a) An enhanced influence of tropical Indian Ocean on the South Asia High after the late 1970s. J Clim 25(20):6930–6941. doi:10.1175/jcli-d-11-00696.1

Qu X, Huang G (2012b) Impacts of tropical Indian Ocean SST on the meridional displacement of East Asian jet in boreal summer. Int J Climatol 32(13):2073–2080. doi:10.1002/joc.2378

Rasmusson EM, Carpenter TH (1982) variations in tropical sea-surface temperature and surface wind fields associated with the southern oscillation El-Nino. Mon Weather Rev 110(5):354–384. doi:10.1175/1520-0493(1982)110<0354:vitsst>2.0.co;2

Rayner NA, Parker DE, Horton EB, Folland CK, Alexander LV, Rowell DP, Kent EC, Kaplan A (2003) Global analyses of sea surface temperature, sea ice, and night marine air temperature since the late nineteenth century. J Geophys Res-Atmos 108(D14):4407 doi: 10.1029/2002jd002670

Schott FA, Xie SP, McCreary JP (2009) Indian Ocean circulation and climate variability. Rev Geophys 47:RG1002 doi: 10.1029/2007rg000245

Sobel AH, Bretherton CS (2000) Modeling tropical precipitation in a single column. J Clim 13(24):4378–4392. doi:10.1175/1520-0442(2000)013<4378:mtpias>2.0.co;2

Su H, Neelin JD, Meyerson JE (2003) Sensitivity of tropical tropospheric temperature to sea surface temperature forcing. J Clim 16(9):1283–1301. doi:10.1175/1520-0442-16.9.1283

Wallace JM (1992) effect of deep convection on the regulation of tropical sea-surface temperature. Nature 357(6375):230–231. doi:10.1038/357230a0

Watanabe M, Kimoto M (2000) Atmosphere–ocean thermal coupling in the North Atlantic: a positive feedback. Q J R Meteorol Soc 126(570):3343–3369. doi:10.1256/smsqj.57016

Weng H, Behera SK, Yamagata T (2009) Anomalous winter climate conditions in the Pacific rim during recent El Niño Modoki and El Niño events. Clim Dyn 32(5):663–674

Wu RG, Yang S, Liu S, Sun L, Lian Y, Gao ZT (2010) Changes in the relationship between Northeast China summer temperature and ENSO. J Geophys Res-Atmos 115:D21107 doi: 10.1029/2010jd014422

Wu RG, Chen JL, Chen W (2012) Different Types of ENSO Influences on the Indian summer monsoon variability. J Clim 25(3):903–920. doi:10.1175/jcli-d-11-00039.1

Xie SP, Annamalai H, Schott FA, McCreary JP Jr (2002) Structure and mechanisms of south indian ocean climate variability. J Clim 15(8):864–878

Xie SP, Hu K, Hafner J, Tokinaga H, Du Y, Huang G, Sampe T (2009) Indian Ocean capacitor effect on Indo-western Pacific climate during the summer following El Niño. J Clim 22(3):730–747

Xie SP, Du Y, Huang G, Zheng XT, Tokinaga H, Hu KM, Liu QY (2010) Decadal shift in El Niño influences on Indo-Western Pacific and East Asian climate in the 1970s. J Clim 23(12):3352–3368. doi:10.1175/2010jcli3429.1